Triple configuration coexistence in ^{44}S

D. Santiago-Gonzalez,[1] I. Wiedenhöver,[1] V. Abramkina,[1] T. Baugher,[2,3] D. Bazin,[2] B. A. Brown,[2,3] P. D. Cottle,[1] A. Gade,[2,3] T. Glasmacher,[2,3] K. W. Kemper,[1] S. McDaniel,[2,3] A. Rojas,[1] A. Ratkiewicz,[2,3] R. Meharchand,[2,3] E. C. Simpson,[4] J. A. Tostevin,[4] A. Volya,[1] and D. Weisshaar[2]

[1] *Department of Physics, Florida State University, Tallahassee, FL, 32306-4350, USA*
[2] *National Superconducting Cyclotron Laboratory, Michigan State University, East Lansing, MI, 48824, USA*
[3] *Department of Physics and Astronomy, Michigan State University, East Lansing, MI, 48824, USA*
[4] *Department of Physics, Faculty of Engineering and Physical Sciences,*
University of Surrey, Guildford, Surrey GU2 7XH, United Kingdom
(Dated: March 21, 2011)

The neutron-rich $N = 28$ nucleus ^{44}S was studied using the two-proton knockout reaction from ^{46}Ar at intermediate beam energy. We report the observation of four new excited states, of which one is a strongly prolate deformed 4^+ state, as indicated by a shell-model calculation. Its deformation originates in a neutron configuration which is fundamentally different from the "intruder" configuration producing the ground state deformation. Consequently, we do not have three coexisting shapes in ^{44}S, but three coexisting configurations, corresponding to zero, one and two neutron particle-hole excitations.

For twenty years, a primary focus of nuclear structure physics has been the search for the proposed modification of shell structure in nuclides near the neutron dripline [1–8]. The neutron shell closures at $N = 28, 50, 82$ and 126 are set by the spin-orbit splitting of high angular momentum orbits, so that a reduction in the splitting would result in the narrowing or collapse of one or more of these shell gaps. The modification of shell gaps has recently been discussed as due to two-body effective interactions of central and tensor type [9] and a decomposition into central, vector and tensor forces [10]. At present, the only one of the spin-orbit based neutron shell closures that is accessible to experiments close to the neutron dripline is $N = 28$, and the narrowing of this gap was recently established experimentally [11–13].

Experimental investigations of how the narrowing of the $N = 28$ gap affects nuclear structure have been focused on how two particle–two hole "intruder" configurations resulting from the promotion of a pair of neutrons across the $N = 28$ gap cause deformation in these nuclei. The recent study of the ground state and excited 0^+ state in ^{44}S [14] highlights the interaction between the "normal" configuration - in which the neutrons are confined to the orbits below the $N = 28$ gap - and the intruder configuration.

In this paper we report on the observation of a 4^+ state at 2447 keV, populated via the two-proton knockout reaction from ^{46}Ar performed at intermediate energies, as well as three other states and five γ-transitions that were previously unobserved. The spin and parity assignment for the 2447 keV state is made using the longitudinal momentum distribution of the projectile residues. A shell model calculation performed using the new SDPF-U effective interaction [15] suggests that this state is strongly deformed and that the neutron configuration responsible for this deformation results from promotion of a single neutron across the $N = 28$ gap - a fundamentally different microscopic mechanism than that which causes de-

formation in the "intruder" 0^+ ground state. The shell model calculation also provides a prediction that this deformed 4^+ state has a half-life of approximately 60 ps, giving it a character that is generally associated with the term "high-K isomer" in heavier nuclei. Thus, ^{44}S does not have three coexisting shapes, but three coexisting configurations, corresponding to zero, one and two-neutron particle-hole excitations.

The present experiment was performed at the National Superconducting Cyclotron Laboratory at Michigan State University using the Coupled Cyclotrons Facility (CCF). A beam of the radioactive isotope ^{46}Ar was produced via fragmentation of a primary beam of 140 MeV/nucleon ^{48}Ca provided by the CCF. The primary beam was fragmented on a 705 mg/cm^2 thick beryllium target, and the fragmentation products were separated in the A1900 fragment separator [16]. The separator selected a secondary beam of 99.9 MeV/nucleon ^{46}Ar which had a momentum spread of $\pm 1.3\%$ and a purity greater than 90%. The rate of ^{46}Ar particles impinging on the secondary target averaged 7×10^5 particles/s.

The knockout reactions were induced on a secondary beryllium target of thickness 188 mg/cm^2. The residual projectile-like nuclei were detected in the S800 spectrograph [17]. Figure 1 shows the histogram of signals used to identify the reaction residues. Gamma -rays emitted at the secondary target location were detected using the SeGA array of 17 segmented germanium detectors [18] in coincidence with the residues in the S800 spectrograph. The total photopeak efficiency of the SeGA array for γ-rays emitted in-flight (v/c = 0.4211) was 2.5% at 1 MeV and 1.4% at 2 MeV.

The γ-ray spectrum in coincidence with the ^{44}S residual nuclei is shown in Fig.2. These spectra are Doppler-reconstructed so that they appear as in the rest frames of the residual nuclei. The strongest γ-ray in the spectrum is the 1319 keV line, which was was first observed in 1997 by Glasmacher *et al.* in a measurement of the in-
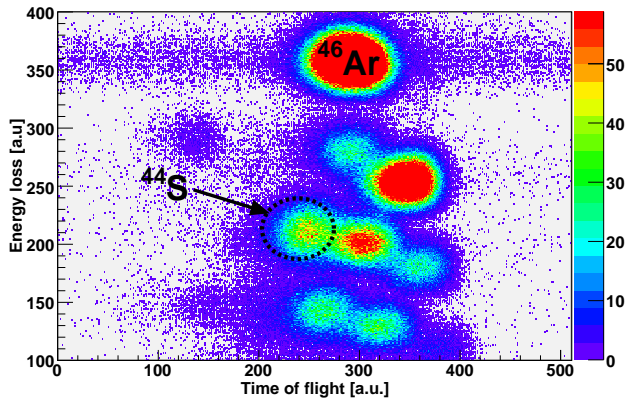
FIG. 1: Spectrum of residual nuclei identified in the S800 spectrograph. The particles labeled ^{46}Ar correspond to scattered beam particles in the hydrogen-like charge state. The vertical axis displays the energy loss of nuclides measured in the focal plane, and the horizontal axis represents a path-corrected time–of–flight signal measured between a focal plane detector and the accelerator RF reference.

termediate energy Coulomb excitation reaction [19] and assigned to be the $2^+_1 \rightarrow 0^+_{gs}$ transition. In addition, we observe γ–rays at 949, 1128, 1891, 1929 and 2150 keV. The experimental uncertainties on the γ-ray energies are 0.5%.

Fig.3 shows the spectrum of γ-rays in coincidence with both the 1319 keV γ-ray and the ^{44}S residues. This coincidence spectrum shows three of the peaks from Fig.2, at 949, 1128 and 1929 keV. On this basis, we establish the existence of states at 2268, 2447 and 3248 keV. The coincidence spectra gated on the 949 and 1128 keV and 1929 keV γ rays show no mutual coincidences. The level scheme we deduce is shown in Fig.4.

Fig.2 also shows two γ-rays at 1891 and 2150 keV that are not seen in the 1319 keV coincidence spectrum. With respect to the 1891 keV γ-ray, we note that Force et al. [14] previously reported the observation of an isomeric 0^+ state at 1365(1) keV, which is 36 keV above the energy they assigned for the 2^+_1 state, 1329(1) keV. The only decay of this state would be to the ground state via the emission of conversion electrons, so this decay could not be observed in the present experiment. However, the 1891 keV γ-ray is 38 keV lower in energy than the 1929 keV γ-ray that deexcites the 3248 keV state. Hence, we tentatively assign the 1891 keV γ-ray as a transition from the 3248 keV state to the 0^+_2 state proposed by Force et al.. Within the statistical limits of our experiment, the 2150 keV γ-ray is not coincident with other γ–rays and is, thus, tentatively placed populating the ground state. Table I lists the levels, cross sections for populating these levels, the gamma-rays deexciting the levels and their intensities.

Sohler et al. published a level scheme for ^{44}S deduced from γ-rays observed during the fragmentation of an intermediate energy beam of ^{48}Ca [20]. The only γ-transition that is unambiguously common to the spectra
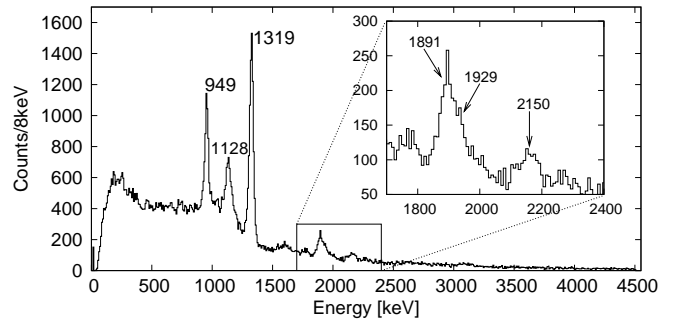

FIG. 2: Doppler-corrected ($v/c = 0.4211$) energy of γ-rays detected in coincidence with the ^{44}S residues. Inset shows a close-up of the 1700-2400 keV region where three less intense photopeaks are identified.
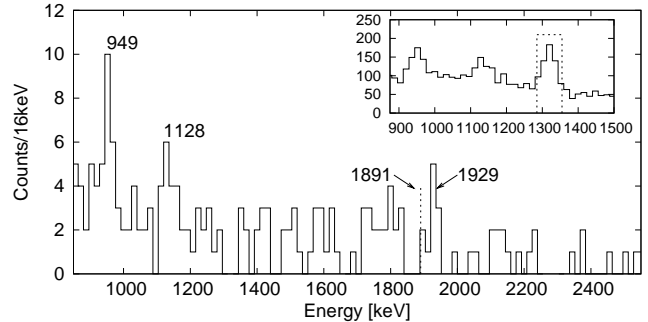

FIG. 3: Doppler-corrected energy of γ-rays detected in coincidence with the 1319 keV γ-rays emitted from a ^{44}S nucleus. Inset: Projected spectrum of $\gamma\gamma$ events showing energy coincidence window in dotted lines.

of Sohler et al. and the present work is the $2^+_1 \rightarrow 0^+_{gs}$ transition, which Sohler quotes as 1350(10) keV and which is quoted as 1319(7) keV here. Sohler et al. also assign a 988(15) keV transition to ^{44}S and say that it deexcites a state at 2632 keV. There is a 31 keV difference between the 2^+_1 state energies quoted here and by Sohler et al., so it is possible that the 949(5) keV γ-ray observed here is identical to the 988(15) keV γ-ray reported by Sohler et al.. However, if the two γ-rays are identical, it is clear that the γ-ray was misplaced in the level scheme in the previous study.

Longitudinal momentum distributions were extracted for residues in coincidence with the 949 and 1128 keV γ-transitions, corresponding to the direct population of the 2268 keV and 2447 keV levels. In addition, a distribution was extracted for residues from direct population of the 1319 keV state by proportionally subtracting the distributions in coincidence with the 949 and 1128 keV γ-transitions from the one in coincidence with the 1319 keV γ–rays. In Fig.5, the observed distributions are compared with those calculated for states of different J^π values, which were corrected for the broadening induced by beam particle and reaction residue energy losses in the target. The model used for calculating these distributions assumes sudden, direct two-proton removal reactions and combines eikonal dynamics and shell model

wavefunctions. These shell model calculations were performed using the SDPF-U interaction [15], which was recently deduced from a fit to data on $Z = 8 - 20$ nuclei ranging from near-proton dripline to near-neutron dripline systems.

The reaction theory, first presented in Refs. [22, 23] and extended in [24, 25], demonstrates that the reaction dynamics restrict direct two-nucleon removal events to grazing collisions. In this way the collision samples the joint position and momentum configurations of the two removed nucleons [26]. Here, the shell model calculations provide the two-proton amplitudes connecting the ground state of the parent nucleus (^{46}Ar) with the final states of the daughter nucleus (^{44}S). In general, a wider longitudinal momentum distribution indicates a higher total and orbital angular momentum transfer to the residual nucleus. The momentum distribution for the 1319 keV state is consistent with an assignment of 2^+ that was set in Ref. [19]. The observed distribution in coincidence with the 949 keV γ-ray is also best reproduced by a 2^+ assignment for the 2268 keV state. However, the experimental distribution in coincidence with the 1128 keV γ–ray indicates a 4^+ assignment for the 2447 keV state.

Fig.4 compares the states observed in the present experiment with predictions of the shell model calculation. The experimental results are also listed in table I. The calculation predicts five excited states below 2.7 MeV in agreement with our observations. The predictions of γ–ray intensities, represented by arrow widths in Fig.4 (right), are derived from the calculated cross sections for the direct population of the excited states and their corresponding γ–decay branches, where we used the effective charges $e_p = 1.5$ and $e_n = 0.5$ and the free-nucleon M1 operator.

The inclusive cross section of the 2-proton knockout reaction is 0.23(2) mb, while the reaction model calculates 0.87 mbarn. These observed cross sections are smaller than those calculated with the shell model and reaction model. However, theoretical cross sections systematically overestimate experimental cross sections by a factor of 2 [23] and the present results do not deviate significantly from this reduction.

Table I also lists the individual experimental and calculated cross sections for the observed states. The ground state and the excited 0^+ states are calculated to carry more than 50% of the total cross section. Among the excited states populated in our experiment, the 2_3^+ and 4_1^+ carry the largest individual cross sections, larger than the 2_1^+, which, in agreement with the calculation, is populated mostly indirectly. The tentatively identified 2150 keV (2_2^+) state is only weakly populated, while the reaction model predicts a strong population. It is interesting to note that the unobserved rotational 4_2^+ state, is calculated to be populated with less than 1 μb of cross section.

The role of the two particle–two hole (2p 2h) neutron intruder configurations in inducing deformation in ^{44}S was first illustrated by Glasmacher *et al.* [19] who ob-

E_{level} [keV]	J^π	E_γ [keV]	J^π_{final}	σ [mb]	σ_{theory} [mb]
0	0^+				0.334
1319(7)	2_1^+	1319(7)	0_1^+	0.014(3)	0.028
1357(15)	0_2^+				0.163
2150(11)*	(2_2^+)	2150(11)	0_1^{+*}	0.004(1)	0.076
2268(8)	2_3^+	949(5)	2_1^+	0.022(4)	0.082
2447(9)	4_1^+	1128(6)	2_1^+	0.019(4)	0.032
3248(12)	(2_4^+)	1891(10)	0_2^{+*}	0.011(3)	0.033
		1929(7)	2_1^+		

TABLE I: Deduced energy levels of ^{44}S, E_{level}, with their spin and parity, J^π, cross section, σ, measured de-excitation energy of γ-ray, E_γ placed towards the final level. Tentative placements are marked with an asterisk*.

served a large $B(E2 \uparrow)$ value of 314(88) $e^2 fm^4$ (6.8(20) Weisskopf units), implying significant collectivity or permanent quadrupole deformation. The recent electron spectroscopy studies of Grevy *et al.* [21] and Force *et al.* [14] demonstrated that the 0_1^+ ground state and the excited 0_2^+ state represent a strongly mixed two–state system based on the prolate deformed intruder 2p 2h neutron configuration and spherical state originating in the normal neutron configuration.

The shell model calculation of this work gives a large laboratory frame electric quadrupole moment, 26 efm^2, for the lowest 4^+ state observed in the present experiment. However, this 4^+ state is not connected to the deformed ground state band by the strong $E2$ transitions that would be characteristic of in-band transitions. Instead, the calculation predicts that the 4^+ state is de-excited by a hindered $E2$ transition to the 2_1^+ so that it has a long lifetime - about 60 ps. In fact, in a heavier rotational nucleus this 4^+ state would be called a "high-K" isomer because it appears to be the band head of a $K = 4$ band. If we transform the shell model result for the quadrupole moment of this state to an intrinsic frame (using a rotational model and the $K = 4$ hypothesis), we find that the intrinsic deformation is prolate with a magnitude of 51 efm^2.

While the ground state band is calculated with a prolate deformation as well, the microscopic origins of these prolate deformations are quite different. An examination of the lowest 4^+ state reveals that it is mainly based on 1p 1h neutron excitations, accounting for 59% of its wave function with $(f_{7/2})^{-1} p_{3/2}$ as the leading configuration. By comparison, the rotational 2_1^+ and 4_2^+ shell model states are dominated by 2p 2h excitations with 63% and 65% of their respective wave functions. It is interesting to note that the 4_1^+ and the un-observed rotational 4_2^+ state are calculated to be separated by only 164 keV, yet exhibit virtually no mixing, as demonstrated by the long calculated lifetime of the 4_1^+. Thus, we do not have three coexisting shapes in ^{44}S, but three coexisting configurations, corresponding to zero, one and two neutron particle-hole excitations.

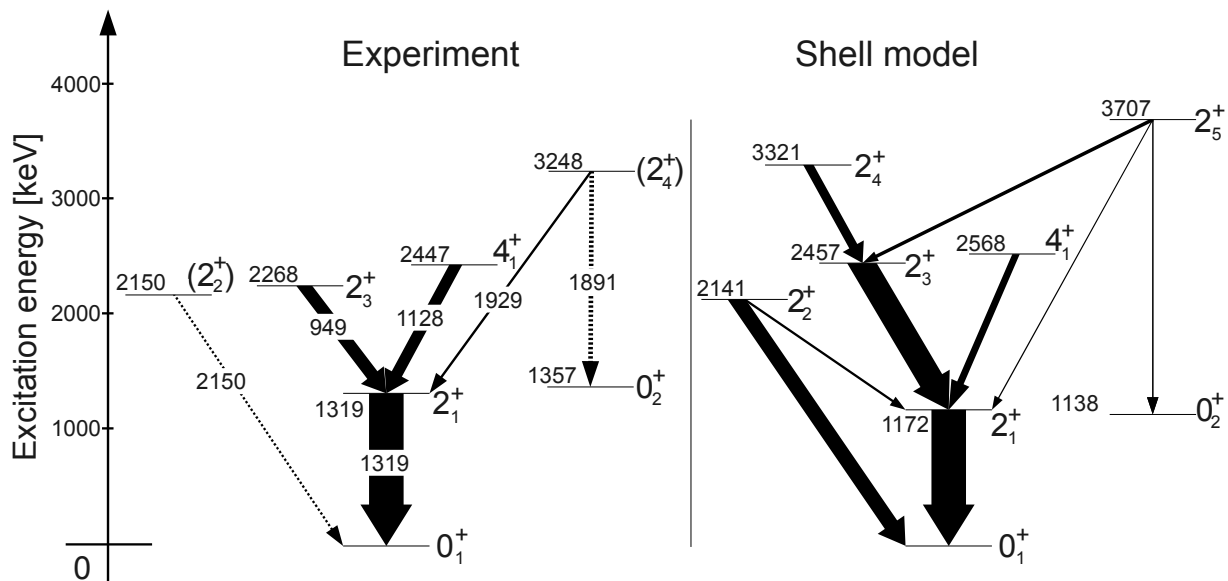The line shape of the 1128 keV γ-ray is suggestive of a

FIG. 4: (Left) Experimental ^{44}S level scheme. The arrow widths are proportional to the observed intensity of the transitions. (Right) Level and transition scheme predicted by the shell model (see text). The arrow widths represent the calculated γ–intensities based on population cross sections and subsequent γ–decay branching ratios, normalized to the strength of the $2_1^+ \rightarrow 0_1^+$ transition. We show all predicted transitions calculated larger than 3% of the ground state transition intensity.

broadened shape, consistent with simulations of a delayed emission with a mean life around 50 ps. However, the effects are not strong enough to provide evidence. Proof of a delayed emission will have to come from a Recoil-Distance Method measurement. Such a measurement would provide a strong confirmation of the deformed nature of this state, its seperate microscopic configuration and, thus, triple configuration coexistence in this nuclide.

In summary, we have examined configuration coexistence in ^{44}S using the two proton knockout reaction from ^{46}Ar at intermediate energy. Four new excited states were observed. Two new spin assignments were made based on the longitudinal momentum distributions of the projectile residues. The observed states include a 4^+ state at 2447 keV. A shell model calculation using the SDPF-U interaction suggests that this state has a strong prolate deformation in both the lab and intrinsic frames, but that its deformation is based on a neutron 1p 1h configuration which is different from the neutron 2p 2h intruder configuration responsible for the ground state deformation of this nucleus. A Recoil Distance Method measurement of the lifetime of the 2447 keV 4^+ state could confirm its deformed nature and the presence of triple configuration coexistence within 2.4 MeV in ^{44}S.

[1] T. R. Werner *et al.*, Phys. Lett. **B333**, 303 (1994).
[2] T. R. Werner *et al.*, Nucl. Phys. A **597**, 327 (1996).
[3] J. Terasaki,H. Flocard, P.-H. Heenen, and P. Bonche, Nucl. Phys. **A621**, 706 (1997).
[4] G. A. Lalazissis, A. R. Farhan, and M. M. Sharma, Nucl. Phys. *A628*, 221 (1998).
[5] G. A. Lalazissis, D. Vretenar, P. Ring, M. Stoitsov, and L. Robledo, Phys. Rev. C **60**, 014310 (1999).
[6] S. Peru, M. Girod, and J. F. Berger, Eur. Phys. J. A **9**, 35 (2000).
[7] R. Rodriguez-Guzman, J.L. Egido, and L.M. Robledo, Phys. Rev. C **65**, 024304 (2002).
[8] J. Piekarewicz, J. Phys. G **34**, 467 (2007).
[9] T. Otsuka *et al.*, Phys.Rev.Lett. **104**, 012501 (2010)
[10] N.A. Smirnova *et al.*, Physics Letters **B 686**, 109 (2010)
[11] C.M. Campbell *et al.*, Phys. Rev. Lett. **97**, 112501 (2006).
[12] B. Bastin *et al.*, Phys. Rev. Lett. **99**, 022503 (2007).
[13] L.A. Riley *et al.*, Phys. Rev. C **78**, 011303(R) (2008).
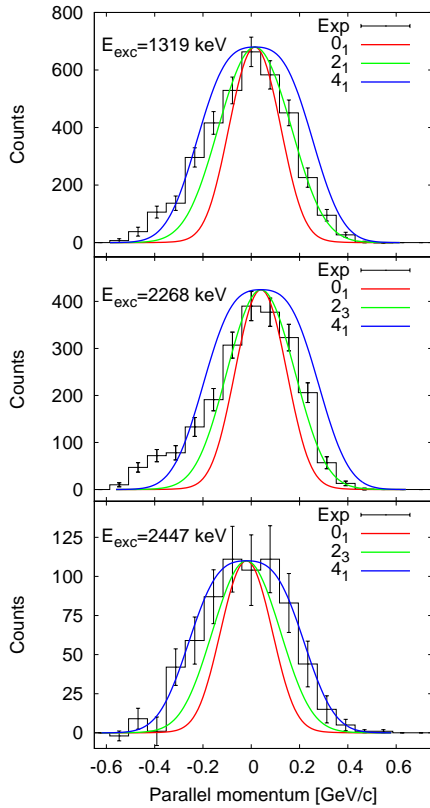[14] C. Force *et al.*, Phys. Rev. Lett. **105**, 102501 (2010).

FIG. 5: (color online) Calculated and observed longitudinal momentum distributions for the direct population of the 1319 keV state (2_1^+) (top), the 2268 keV state (2_3^+) (middle) and the 2447 keV state (4_1^+) (bottom). The experimental histogram is compared to the distributions calculated from the two-proton knockout mechanism for different final state spin hypotheses (see text).

[15] F. Nowacki and A. Poves, Phys. Rev. C **79**, 014310 (2009).

[16] D.J. Morrissey *et al.*, Nucl. Instrum. Methods Phys. Res. B **204**, 90 (2003).

[17] D. Bazin *et al.*, Nucl. Instrum. Methods Phys. Res. B **204**, 629 (2003).

[18] W.F. Mueller *et al.*, Nucl. Instrum. Methods Phys. Res. A **466**, 492 (2001).

[19] T. Glasmacher *et al.*, Phys. Lett. B **395**, 163 (1997).

[20] D. Sohler *et al.*, Phys. Rev. C **66**, 054302 (2002).

[21] S. Grevy *et al.*, Eur. Phys. J. A **25**, s01, 111 (2005).

[22] J.A. Tostevin, G. Podolyak, B.A. Brown, and P.G. Hansen, Phys. Rev. C **70**, 064602 (2004).

[23] J.A. Tostevin and B.A. Brown, Phys. Rev. C **74**, 064604 (2006).

[24] E.C. Simpson, J.A. Tostevin, D. Bazin, B.A. Brown, and A. Gade, Phys. Rev. Lett. **102**, 132502 (2009).

[25] E. C. Simpson, J. A. Tostevin, D. Bazin, and A. Gade, Phys. Rev. C **79**, 064621 (2009).

[26] E.C. Simpson and J.A. Tostevin, Phys. Rev. C **82**, 044616 (2010)